Lithium Intercalation into Monoclinic Cr_4TiSe_8: Synthesis, Structural Phase Transition, and Properties of $Li_xCr_4TiSe_8$ ($x = 0.1-2.8$)

Malte Behrens,[†] Oliver Riemenschneider,[†] Wolfgang Bensch,*[,†] Sylvio Indris,[‡] Martin Wilkening,[‡] and Paul Heitjans[‡]

Institute of Inorganic Chemistry, University of Kiel, Olshausenstrasse 40−60, 24098 Kiel, Germany, and Institute of Physical Chemistry and Electrochemistry, University of Hannover, Callinstrasse 3−3a, 30167 Hannover, Germany

Received August 18, 2005. Revised Manuscript Received November 15, 2005

The intercalation reaction of Li into the complex ternary selenide Cr_4TiSe_8 was investigated as function of time and temperature. The treatment of the host compound with a solution of butyl lithium in *n*-hexane (BuLi) leads to Li insertion up to the composition $Li_{2.8}Cr_4TiSe_8$. The intercalation reaction is accompanied by a structural phase transition of the host material. The monoclinic symmetry of pristine Cr_4TiSe_8 is changed to trigonal when x in $Li_xCr_4TiSe_8$ exceeds approximately 0.4. With increasing Li content the axes of the new trigonal unit cell are significantly enlarged. The structural phase transition was characterized by Rietveld refinement of X-ray (XRD) powder patterns for different values of x. The phase transition is electronically driven rather than being due to geometric reasons. Immediately after removal of the excess BuLi of partially intercalated phases, the product is not in equilibrium and undergoes a structural relaxation. When the lithiated products are treated with water, the intercalated Li is removed while the symmetry does not switch back from trigonal to monoclinic. The final composition of the deintercalated samples was always $Li_{\approx 0.4}Cr_4TiSe_8$. The strain of the samples introduced by the Li insertion and the phase transition was investigated with line profile analysis (LPA) of the XRD patterns. The intercalation reaction is accompanied by a strong increase of the strain. Static ^{7}Li NMR measurements of the fully intercalated sample $Li_{2.8}Cr_4TiSe_8$ show a broad line due to the strong interaction of the Li nuclei with the Cr ions. ^{7}Li magic angle spinning (MAS) NMR studies reveal the presence of two nonequivalent Li sites.

Introduction

Lithium intercalation compounds have drawn a lot of attention during the past decades, because of their possible application as electrode materials in alkali metal batteries.[1−6] Formally, the host compounds are reduced during the intercalation process as they accept an electron from elemental Li (discharging the battery), or they are oxidized as Li is deintercalated (charging the battery). Investigations of intercalation reactions of transition metal dichalcogenides (TMDC) played an important role in understanding fundamental steps of intercalation processes. TMDC's (MX_2 with M = transition metal of groups 4−6, X = S, Se) as host lattices have been of particular interest because of their ability to isomorphously substitute M and/or X. Alkali metal intercalation in the van der Waals gaps between MX_2 layers results in an enlargement of the interlayer distance. Structural phase transitions and changes of the electronic properties may occur during the intercalation process and have been extensively investigated. Systematic studies revealed a relation of structural and electronic features in a given series of A_xMX_2 compounds (A = alkali metal).[7−12] Some TMDC's are also suitable electrode materials for Li batteries.[6,13]

Most of the transition metal chalcogenides M_yX_z with M:X ratios > 0.5 exhibit a three-dimensional structure. In these compounds void spaces are often present in the form of tunnels, and examples of intercalation of guests in such 3D hosts are well-known.[14−16] The chromium chalcogenide Cr_5Se_8, which also crystallizes in a 3D structure with accessible

* To whom correspondence should be addressed. Telephone: +49 431 880-2406. Fax: +49 431 880-1520. E-mail: wbensch@ac.uni-kiel.de.
[†] University of Kiel.
[‡] University of Hannover.

(1) Murphy, D. W.; Christian, P. A. *Science* **1979**, *205*, 651.
(2) Besenhard, J. O. In *Progress in Intercalation Research*; Müller-Warmuth, W., Schöllhorn, R., Eds.; Kluwer Academic Press: Dordrecht, The Netherlands, 1994.
(3) Winter, M.; Besenhard, J. O.; Spahr, M. E.; Novák, P. *Adv. Mater.* **1998**, *10*, 725.
(4) McKinnon, W. R.; Hearing, R. R. *Mod. Aspect. Electrochem.* **1983**, *15*, 235.
(5) Benco, L.; Barras, J.-L.; Atanasov, M.; Daul, C.; Deiss, E. *J. Solid State Chem.* **1999**, *145*, 503.
(6) Abrahan, K M.; Pasquariello, D. M.; Schwartz, D. A. *J. Power Sources* **1989**, *26*, 247.
(7) Brec, R.; Prouzet, E.; Ouvrard, G. *J. Power Sources* **1993**, *43*, 277.
(8) Molinié, P.; Trichet, L.; Rouxel, J.; Bertier, C., Chabre, Y.; Segransan, P. *J. Phys. Chem. Solids* **1984**, *45*, 105.
(9) Whangbo, M. H.; Trichet, L.; Rouxel, J. *Inorg. Chem.* **1985**, *24*, 1824.
(10) Frindt, R. F. *NATO ASI Ser., Ser. B (Chem. Phys. Intercalation, 1987)* **1987**, *172*, 195.
(11) Omloo, W. P. F. A.; Jellinek, F. *J. Less Common Met.* **1970**, *20*, 121.
(12) Brec, R.; Deniard, P.; Rouxel, J. In *Progress in Intercalation Research*; Müller-Warmuth, W., Schöllhorn, R., Eds.; Kluwer Academic Press: Dordrecht, The Netherlands, 1994.
(13) Dominko, R.; Arèon, D.; Mrzel, A.; Zorko, A.; Cevc, P.; Venturini, P.; Gaberscek, M.; Remskar, M.; Mihailoviv, D. *Adv. Mater.* **2002**, *14*, 1531.
(14) Schöllhorn, R. *Angew. Chem., Int. Ed. Engl.* **1980**, *19*, 983.

10.1021/cm0518628 CCC: $33.50
Published on Web 02/21/2006

sites, was shown to be stable only at high pressures and high temperatures.[17,18] It is believed that Cr(IV) is not stable under ambient conditions in an environment of Se or S, and one way to stabilize a compound with the Cr_5Se_8 structure type is the partial substitution of Cr by Ti, which adopts the required oxidation state +IV much easier than Cr. According to this assumption we recently presented the new ternary selenide Cr_4TiSe_8, which is stable at room temperature and could be prepared under ambient pressure.[19] This compound exhibits some interesting features such as an unusual metal atom distribution and magnetic spin glass behavior. The structural relationship of Cr_4TiSe_8 with the TMDC's is obvious, if Cr_4TiSe_8 is treated as a partially self-intercalated compound with formula $(M_1M_{0.25})Se_2$ (M = Cr, Ti). The 0.25 metal atoms per formula unit reside in the "van der Waals gap", leaving the remaining sites within the "gap" free for guest atoms. These void sites in the structure of Cr_4TiSe_8 make this compound a promising host material for intercalation experiments. Furthermore, the electronic structure of Cr_4TiSe_8 allows an intercalation of guest atoms with a simultaneous charge transfer from the guest to the host. Li intercalation in Cr_4TiSe_8 was found to be possible and preliminary results were presented before.[20] Such an intercalation with electron transfer from the guest to the host allows a stepless tuning of the electronic structure of the material. In addition, the intercalation reaction is performed under ambient conditions and is a soft chemistry route for the design of physical properties of new materials. Here, we report on the synthesis, structural properties, and NMR spectroscopic data of the intercalation and deintercalation products $Li_xCr_4TiSe_8$ ($0 < x < 3$).

Experimental Section

Synthesis. The host compound Cr_4TiSe_8 was synthesized from the elements as described elsewhere.[19] Phase purity of the samples was checked with a Rietveld refinement before intercalation, which resulted in R_{Bragg} factors better than 5%. The intercalation reaction was performed in 1.6 M ^{t}BuLi in *n*-hexane (BuLi) as the source of Li in a glovebox with Ar atmosphere. In a typical reaction 50 mg of Cr_4TiSe_8 was suspended in 5 mL of BuLi. This is roughly a molar Li excess of 50:1. The samples were filtered and washed with *n*-hexane after the reaction. To minimize crystallite size effects, the Cr_4TiSe_8 powder was sieved prior to the reaction with a μ-sieve and only the 73−100 μm fraction was used for the intercalation reactions. Note that these particles are agglomerates of small crystallites with a size ranging from 2 to about 15 μm. Reactions at elevated temperatures were performed in a sealed Teflon-lined steel autoclave under Ar atmosphere at 60 °C with typical reaction time of 3 days. Deintercalation was done in demineralized water at ambient temperatures. Samples were collected from the reaction mixture at certain time intervals during intercalation and deintercalation for characterization with X-ray diffraction, scanning electron microscopy, and chemical analysis.

X-ray Diffraction. X-ray diffraction (XRD) data were collected in transmission geometry on a STOE Stadi-P diffractometer equipped with a linear PSD and a Ge monochromator using Cu Kα radiation ($\lambda = 1.54056$ Å). The samples were protected against atmosphere by sealing the sample holder with X-ray transparent foil. Powder patterns were recorded in the 2θ range of 10−90° with a step width of 0.01°. The counting time per step was typically around 1 h. Rietveld refinements of the patterns were done using the program package FULLPROF.[21] The background was treated using linear extrapolation between manually selected points. The reflection profiles were modeled with Thompson−Cox−Hastings pseudo Voigt functions using three parameters. Preferred orientation was accounted for by the March−Dollase function. The zero point was refined as a global parameter.

The line profile analysis (LPA) was performed by single profile fitting of selected, well-resolved reflections using the program package WinXPow.[22] Profiles were modeled with the Pearson VII function. The integral breadths β were corrected for the instrumental line broadening using a powder pattern of LaB_6 as a standard.

Atomic Absorption Spectroscopy. The degree of lithiation of the samples was determined by atomic absorption spectroscopy (AAS) on a Perkin-Elmer AAnalyst 300 device. The sample was dissolved in HNO_3/H_2O_2, and the Li and Se contents were analyzed in several scans. The accuracy was calculated on the basis of the number of analyses to be about 0.5%.

Scanning Electron Microscopy. The morphology of the samples was investigated using scanning electron microscopy (SEM) on a Philips ESEM XL-30.

Nuclear Magnetic Resonance Spectroscopy. ^{7}Li NMR measurements were performed at magnetic fields of 4.7 T (resonance frequency of 78 MHz) and 9.4 T (155 MHz) with Bruker MSL 100 and MSL 400 spectrometers. Static measurements were done in the temperature range from 120 to 450 K. Magic angle spinning (MAS) NMR measurements on ^{7}Li were performed at 155 MHz with a spinning rate of 15 kHz at temperatures between 200 and 360 K. Spectra were referenced to 1 N LiCl aqueous solution.

Results and Discussion

A detailed description of the structure of the host compound was already given elsewhere.[19] A brief introduction of the most important structural details is given in this first short paragraph. Cr_4TiSe_8 crystallizes in the nonconventional space group *F*2/*m* (transformation matrix for *C*2/*m*: (00−1), (010), (0.5 0 0.5)). The lattice parameters are summarized in Table 1. The structure can be derived from the NiAs structure type if metal atoms are removed in an ordered way from every second metal atom layer perpendicular to the crystallographic *c*-axis, yielding empty sites in the structure. There are three crystallographically independent sites for the metal atoms: M1, M2, and M3 (Figure 1a). All metal atoms are in a distorted octahedral environment of six Se atoms. The MSe_6 octahedra in the fully occupied layers (M2 and M3) are connected via common edges, while half of the $M3Se_6$ octahedra share common faces with the $M1Se_6$ octahedra in the partially occupied layers. The metal

(15) James, A. C. W. P.; Goodenough, J. B. *J. Power Sources* **1989**, *26*, 277.
(16) Kriger, Y. G.; Mishenko, A. V.; Semenov, A. R.; Tkachev, S. V.; Fedorov, V. E. *Phys. Solid State* **2000**, *42*, 257.
(17) Sleight, A. W.; Bither, T. A. *Inorg. Chem.* **1969**, *8*, 566.
(18) Huppertz, H.; Lühmann, H.; Bensch, W. *Z. Naturforsch.* **2003**, *58B*, 934.
(19) Bensch, W.; Sander, B.; Näther, C.; Kremer, R. K.; Ritter, C. *Solid State Sci.* **2001**, *3*, 559.
(20) Riemenschneider, O.; Behrens, M.; Bensch, W.; Indris, S.; Heitjans, P. In *Solid State Ionics: The Science and Technology of Ions in Motion*; Chowdari, B. V. R., Yoo, H.-L., Choi, G. M., Lee, J.-H., Eds.; World Scientific Publishing: Singapore, 2004.
(21) Rodriguez-Carvajal, J. *FULLPROF*; Laboratoire Leon Brillouin: Gif-sur-Yvette Cedex, France, 2005.
(22) *ProgramWinXPOW*; STOE GmbH: Darmstadt, Germany, 2001.

Table 1. Structural Data and Details of the Structure Refinement of Cr_4TiSe_8 [19] and $Li_{0.65}CrTi_{0.25}Se_2$ Obtained after 20 day Intercalation in BuLi at Room Temperature

	Cr_4TiSe_8	$Li_{0.65}CrTi_{0.25}Se_2$
a, Å	12.368(2)	3.626(3)
b, Å	7.1808(2)	3.626(3)
c, Å	11.605(2)	6.114(6)
α, deg	90	90
β, deg	91.06(2)	90
γ, deg	90	120
V, Å^3	1030.6(2)	69.648(3)
Z	4	1
crystal system	monoclinic	trigonal
space group	*F*2/*m*	$P\bar{3}m1$
refinement	single crystal:	powder data:
	R1 [a] = 2.15%	R_{Bragg} = 4.52%
	WR2 [a] = 4.61%	R_{wp} = 13.7%
	GOF[b] = 1.012	χ^2 = 3.63

[a] For 619 reflections $F_0 > 4\sigma F_0$. [b] For all reflections.

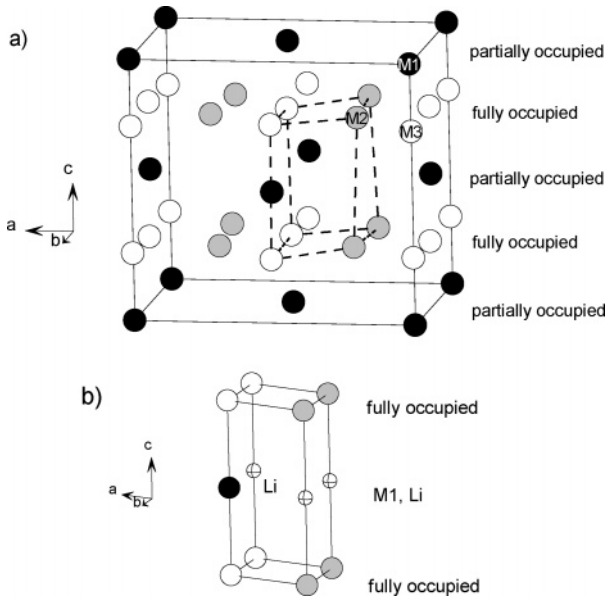

Figure 1. Crystal structure of (a) Cr_4TiSe_8 and (b) $Li_{x'\approx 0.75}CrTi_{0.25}Se_2$. Selenium atoms are omitted for clarity. Different crystallographic metal atom sites are shown in grey, black, and white and metal atom layers are marked as fully occupied or vacant in a. In b the same color scheme for the metal atoms as in a was applied to demonstrate the structural relationship between the two phases.

distribution was determined with neutron scattering experiments, and Ti was found to reside in the fully occupied metal atom layers only (M2 and M3). All M−Se distances are in the normal range. The metal-to-metal separations are 3.299(1) and 3.399(1) and 3.602(1) Å in the fully occupied layer, and due to the face-sharing octahedra the M1−M3 atoms have short contacts of 3.005(1) Å. Such short metal-to-metal distances are typical for chromium chalcogenides.[23−26] For a more detailed discussion of the crystal structure and the magnetic properties of Cr_4TiSe_8 the reader is referred to the reference mentioned above.

The usage of BuLi as Li source was shown to be an easy and elegant route for intercalation experiments on transition

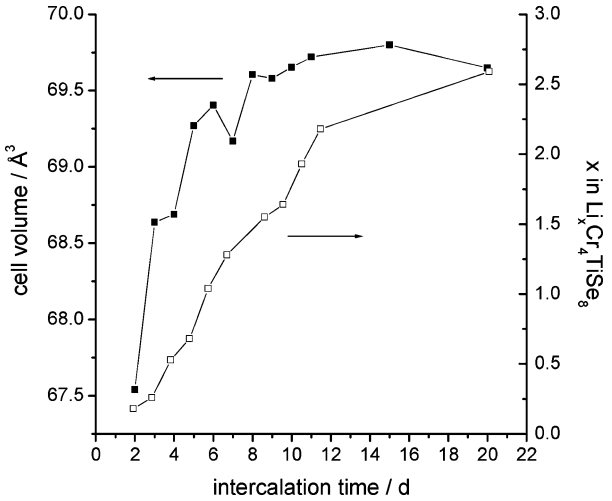

Figure 2. Increase of Li content *x* in $Li_xCr_4TiSe_8$ with intercalation time for an intercalation reaction of Cr_4TiSe_8 in BuLi at room temperature (open symbols) and variation of the unit cell volume of the newly developing phase $Li_{x'}CrTi_{0.25}Se_2$ ($x' = x/4$) (closed symbols). The upper compositional limit with $x = 3$ ($x' = 0.75$) is not reached because the reaction is not complete at room temperature. The lines are guides for the eyes.

metal chalcogenides because the reaction proceeds under ambient conditions.[27−29] The application of a vast excess of Li in the solution exerts a "Li pressure" onto the host material and can be considered as the driving force of the intercalation. One has to keep in mind that this "pressure" stops immediately as the samples are removed from the solution followed by the workup. Directly after the separation of the lithiated phase from the excess BuLi usually nonequilibrated samples are obtained, and a relaxation starts that can be regarded as a room-temperature annealing.[30] This relaxation process will be discussed in detail below.

The reaction of Cr_4TiSe_8 with BuLi at room temperature was interrupted after certain reaction time intervals. It was found to be relatively fast at the beginning and to slow with increasing reaction time (Figure 2). We note that the X-ray data of the sample obtained after 7 days could not be measured directly after the workup due to technical reasons explaining the drop of the unit cell volume, whereas all other XRD patterns were taken immediately to account for the structural relaxation. Even after about 20 days the composition is about $Li_{2.6}Cr_4TiSe_8$, slightly below the limit obtained by reactions at 60 °C, which are much faster, yielding samples with $x = 2.75$ in only 3 days. When *x* becomes larger than approximately 0.4, a structural phase transition from monoclinic to trigonal can be observed in the XRD patterns. The new reflections are indexed on the basis of a trigonal cell with space group $P\bar{3}m1$. Unfortunately, the reactions at room-temperature always yield a mixture of the lithiated product and the genuine material. Figure 3 shows powder patterns of the starting material Cr_4TiSe_8 (Figure 3a), of a sample with both phases (reaction at room temperature, intercalation time 6 days; Figure 3b) and of the intercalated phase obtained after a 3 day treatment with BuLi at 60 °C

(23) Hayashi, A.; Ueda, Y.; Kosuge, K.; Murata, H.; Asano, H.; Watanabe, N.; Izumi, F. *J. Solid State Chem.* **1987**, *67*, 346.
(24) Klepp, K.; Boller, H. *J. Solid State Chem.* **1983**, *48*, 388.
(25) Bensch, W.; Helmer, O.; Näther, C. *J. Solid State Chem.* **1996**, *127*, 40.
(26) Bensch W.; Wörner, E.; Muhler, M.; Ruschewitz, U. *J. Solid State Chem.* **1994**, *110*, 234.
(27) Dines, M. B. *Mater. Res. Bull.* **1975**, *10*, 287.
(28) Whittingham, M. S.; Dines, M. B. *J. Electrochem. Soc.* **1977**, *124*, 1387.
(29) Schöllhorn, R. *Physica B* **1980**, *99*, 89.
(30) Rouxel J. *J. Chim. Phys. Phys.-Chim. Biol.* **1986**, *83*, 841.

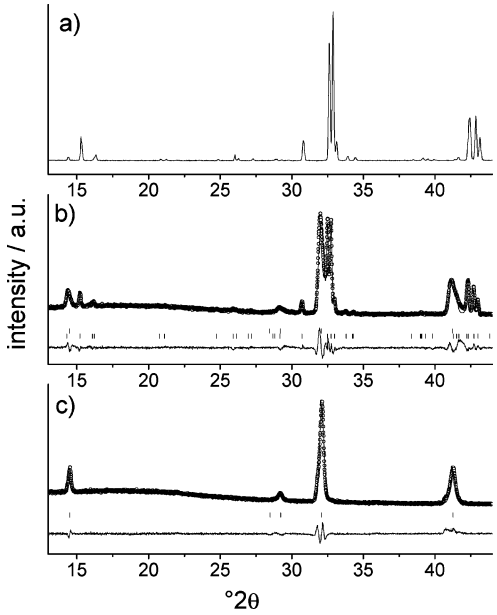

Figure 3. Sections of the powder diffraction patterns of (a) the starting material Cr_4TiSe_8, (b) a phase mixture of Cr_4TiSe_8 and $Li_{x'}CrTi_{0.25}Se_2$ with an average composition $Li_{0.65}Cr_4TiSe_8$ obtained at room temperature, and (c) phase-pure product $Li_{0.69}CrTi_{0.25}Se_2$ obtained at 60 °C. Rietveld refinement was done for b and c. Open circles, experimental data; full lines, fitted pattern; vertical bars:, position of Bragg reflections; bottom curve, difference between measured and fitted data.

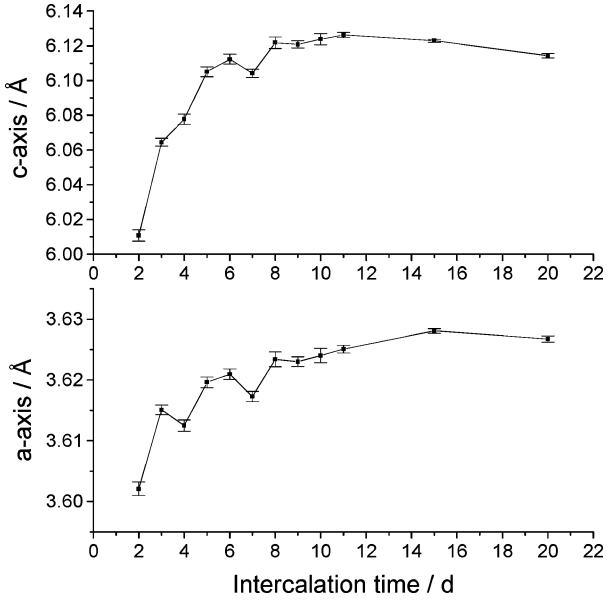

Figure 4. Variation of the lattice parameters of $Li_{x'}CrTi_{0.25}Se_2$ with intercalation time. Note the different scales for the two plots. The *c*-axis is enlarged about three times as much as the *a*-axis. The lines are guides for the eyes.

(Figure 3c). The biphased nature of the room temperature samples is probably due to the relatively slow diffusion of Li in the host. Well-equilibrated single-phase samples $Li_{x>0.4}Cr_4TiSe_8$ with intermediate intercalation degrees can be prepared by the following procedure: The fully intercalated single-phase sample obtained at temperatures above 60 °C is allowed to relax after removal of the excess BuLi. The structural relaxation was found to be much faster for phase-pure trigonal samples than for biphased samples as they are closer to equilibrium from the beginning. No more structural changes were detected after 3 days. The Li content can then be adjusted by deintercalation in water. The deintercalation is discussed later in more detail. The lattice parameters of the host material and the intercalated phase were determined by Rietveld refinements, and the results are summarized in Table 1. The evolution of the lattice parameters of the trigonal phase with intercalation time is shown in Figure 4. Both the *a* and *c* axes as well as the unit cell volume are enlarged with increasing Li content. For the first 6 days a pronounced increase of the cell volume with time is observed which significantly slows down at longer intercalation times. From a crystallographic point of view the trigonal reaction product should be formulated as $Li_{x'=0.69}CrTi_{0.25}Se_2$ rather than $Li_{x=2.75}Cr_4TiSe_8$ ($x' = x/4$), demonstrating the relation to TMDC's mentioned already in the Introduction. The relations between the axes are as follows: $a(Cr_4TiSe_8) \approx 2\sqrt{3}a(Li_{x'\approx 0.75}CrTi_{0.25}Se_2)$, $b(Cr_4TiSe_8) \approx 2a(Li_{x'\approx 0.75}CrTi_{0.25}Se_2)$, and $c(Cr_4TiSe_8) \approx 2c(Li_{x'\approx 0.75}CrTi_{0.25}Se_2)$.

The crystal structure of the developing trigonal $Li_{x'}CrTi_{0.25}Se_2$ phase is shown in Figure 1b. The cell is outlined in Figure 1a in the unit cell of monoclinic Cr_4TiSe_8 to demonstrate the close structural relationship between the two phases. In the structural model used for the Rietveld refinements Li atoms were not considered. In the TMDC-like structure, the M2/M3 atoms of the monoclinic phase are structurally equal and form the fully occupied layer of the trigonal phase (Figure 1). The M1 atom is located in the van der Waals gap together with the Li^+ ions. It can be assumed that the M1 atom is not mobile and the true cell of the intercalated phase should be larger than that used for the refinements. But in the powder patterns no additional reflections were found indicating a superstructure. Hence, in the discussion of the experimental results the structural model applied for the Rietveld refinements is used.

The MSe_6 octahedra are less distorted in $Li_{x'}CrTi_{0.25}Se_2$ than in Cr_4TiSe_8, with all angles being near the ideal values. The M−Se distances in the fully intercalated material are 2.646(1) Å for octahedra located in the partially occupied metal atom layers and 2.514(1) Å for octahedra in the full metal atom layers, which is on average 0.048 Å longer than in Cr_4TiSe_8. The M−M distances within the full layers measure 3.625(1) Å, and the interlayer distance is 3.057(1) Å.

In the monoclinic host structure the intralayer M−M separations are 3.299, 3.399, and 3.602 Å (average, 3.460 Å). In the intercalated material the intralayer M−M distance of 3.625 Å is about 4.7% longer than the average distance in the pristine compound, and the interlayer distance is expanded by roughly 2%. In this respect the system does not behave like a layered phase where the main lattice parameter expansion upon intercalation is usually found perpendicular to the layers.[31] This is clearly the effect of the Cr atoms in the van der Waals gap, which pins the layers together by Cr−Se interactions. Nevertheless, also a weak intralayer expansion was observed in TMDC's which can be attributed mainly to electronic effects. A strong elongation of the intralayer Cr−Cr distance was found for the intercalation of K in $CrSe_2$.[32] The Cr−Cr separation is 0.2 Å longer in $KCrSe_2$ than in $K_{0.6}CrSe_2$. This effect was attributed to

(31) Whittingham, M. S. *Prog. Solid State Chem.* **1978**, *12*, 41−99.

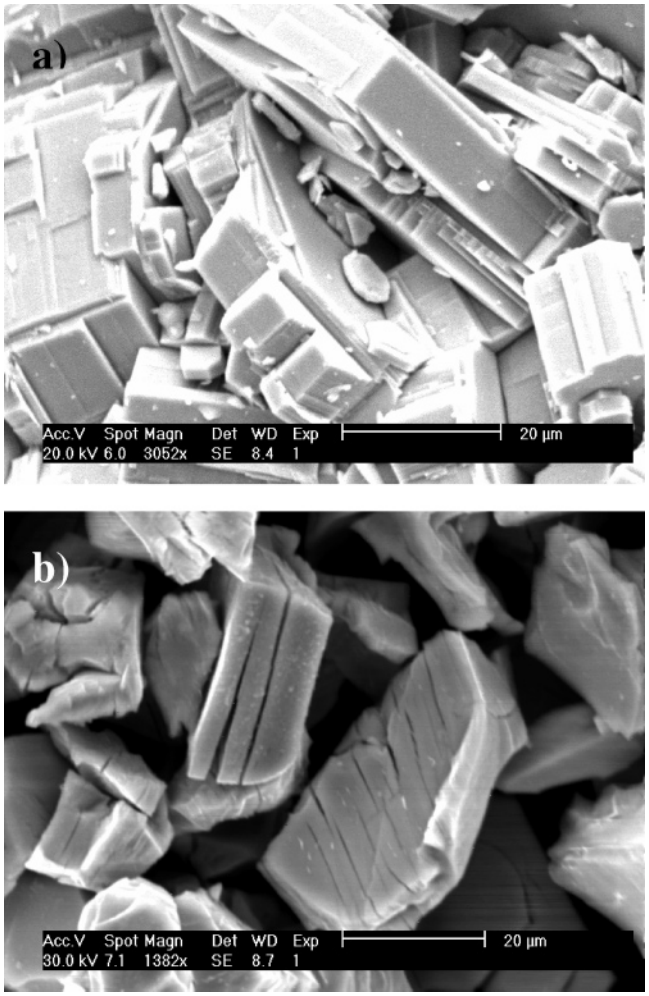

Figure 5. SEM micrographs of the starting material Cr_4TiSe_8 (a) and the lithiated phase $Li_xCrTi_{0.25}Se_2$ (b).

the increasing number of d electrons localized on the Cr centers and the resulting stronger repulsion. In the Cr_4TiSe_8/$Li_xCrTi_{0.25}Se_2$ system an increase of the M−M distance in the full metal atom layers is observed, which is a hint that the main redox centers of the host are located in the fully occupied metal atom layers and that electrons are transferred from Li to these centers during the intercalation process. It cannot be decided from the XRD results whether Ti or Cr or both are reduced by the Li intercalation. First electrochemical results strongly suggest that Ti is reduced first.[33]

The Li atoms could not be located, but it can be assumed that the Li atoms reside in octahedral voids. Another possibility is that Li^+ is located in tetrahedral sites. However, this is not very likely because very short intralayer $Li^{tetr.}$−Cr contacts of 2.245(1) Å would result. Due to the electrostatic repulsion between Cr^{3+} and Li^+, the octahedral sites should be favored. The shortest $Li^{oct.}$−Cr/Ti distance is then 3.057(1) Å.

As noted above the platelike crystals of the starting material measure typically 2 to about 15 μm (Figure 5a), and an interesting observation is that during the intercalation reaction the crystal morphology significantly changes. SEM

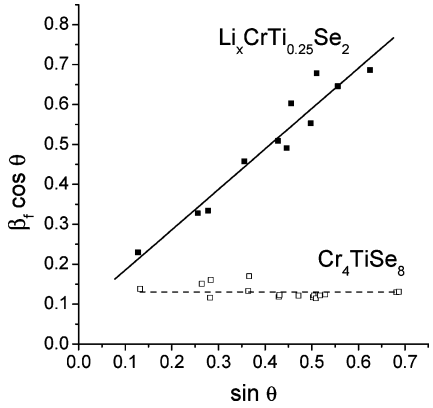

Figure 6. Williamson−Hall plot to identify the nature of line broadening introduced by Li intercalation in Cr_4TiSe_8. Open squares, reciprocal integral breadths β^* for selected, well-resolved reflections of Cr_4TiSe_8; dashed line, the fit; full squares:, β^* for selected, well-resolved reflections of $Li_xCrTi_{0.25}Se_2$; full line, the linear fit.

investigations reveal that after the intercalation reaction the crystals exhibit pronounced damages (Figure 5b). The crystallites show cleavages which are parallel to the lateral extension of the crystals; i.e., they are orientated perpendicular to the *c*-axis resembling typical TMDC materials and demonstrating the structural relationship of Cr_4TiSe_8 to the TMDC's.

In the X-ray powder patterns of the newly developing trigonal phase a pronounced reflection profile broadening compared to the starting material is obvious (Figure 3). A line profile analysis (LPA) was applied to identify the microstructural effects that might contribute to the broadening.[34] The nature of the broadening is then identified from a Williamson−Hall (W−H) plot (Figure 6).[35] The data for the reflections of the starting material Cr_4TiSe_8 are on a horizontal line, indicating that strain can be neglected. This is a typical result for a material prepared at high temperature. The apparent size of coherent diffracting domains determined by the W−H plot is about 626 Å. On the other hand, the data points of the intercalated trigonal phase are on a straight line with a positive slope, indicating that the line broadening is due to a pronounced isotropic strain effect. Semiquantitative evaluations applying the Wilson equation[36] show that the strain is increased by a factor of approximately 10 during the intercalation process. The large amount of strain present in the lithiated product is visible in the SEM micrographs showing cracks and further damage on the surface (Figure 5b). According to the LPA the average apparent crystallite size of the intercalated material is about 533 Å. This reduction by roughly 15% compared to the starting material might be a result of the cleavage of the crystals introduced by the strain.

An interesting observation suggests that the reaction products are not in full equilibrium when the intercalation is stopped. In the powder patterns of samples at intermediate Li concentrations and after removal of the excess BuLi a significant shift of the reflections of the lithiated trigonal phase to higher scattering angles with time is observed, being

(32) Wiegers, G. A. *Physica B* **1980**, *99*, 151.
(33) Behrens, M.; Kiebach, R.; Riemenschneider, O.; Bensch, W. *Chem. Eur. J.*, accepted.
(34) Langford, J. I.; Louer, D.; Sonneveld, E. J.; Visser, J. W. *Powder Diffr.* **1986**, *1*, 211.
(35) Williamson, G. K.; Hall, W. H. *Acta Metall.* **1954**, *1*, 22.
(36) Stokes, A. R.; Wilson, A. J. C. *I. Proc. Phys. Soc.* **1944**, *56*, 174.

Table 2. Selected Results of the Two-Phase Rieveld Refinement of a Sample Containing a Mixture of Cr_4TiSe_8 and $Li_{x'}CrTi_{0.25}Se_2$ Immediately after Intercalation and after a 6 Week Storage and of a Phase-Pure Trigonal Equilibrated Sample[a]

	"$Li_{0.65}Cr_4TiSe_8$"				
	m-Cr_4TiSe_8		*t*-$Li_xCrTi_{0.25}Se_2$		$Li_{0.19}CrTi_{0.25}Se_2$ ($Li_{0.75}Cr_4TiSe_8$)
	immediately	6 weeks	immediately	6 weeks	
R_{Bragg}, %	8.7	10.2	4.84	7.03	9.92
a, Å	12.383(1)	12.384(2)	3.6224(4)	3.6096(8)	3.6039(4)
b, Å	7.191(7)	7.1918(9)			
c, Å	11.63(1)	11.637(2)	6.115(1)	6.012(3)	6.025(1)
β, deg	90.982(5)	90.970(8)			
V, Å^3	1036.03(4)	1036.37(5)	69.501(4)	67.846(7)	67.769(3)
M1−M3, Å	2.82(1)	2.94(2)	no significant variation of atomic coordinates		
M2−M2, Å	3.17(2)	3.37(2)			

[a] The average compositions were $Li_{0.65}Cr_4TiSe_8$ and $Li_{0.75}Cr_4TiSe_8$, respectively.

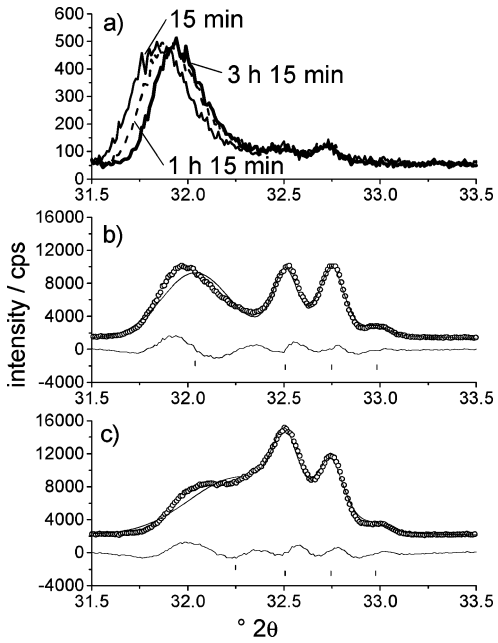

Figure 7. In-situ XRD patterns of the (101) reflection in $Li_{x'\approx0.75}CrTi_{0.25}Se_2$ (a). Rietveld refinement of a sample with coexisting Cr_4TiSe_8 and $Li_{x'}CrTi_{0.25}Se_2$ immediately after intercalation (b) and after a 6 week storage (c). Average composition: $Li_{0.65}Cr_4TiSe_8$. Selected results are summarized in Table 2. Only the fingerprint region of the XRD pattern from 31.5 to 33.5° 2θ is shown. Open circles, experimental data; full lines, fitted pattern; bottom curve, difference between measured and fitted data; vertical bars, position of Bragg reflections.

indicative of a relaxation of the system. The position of the most intense (101) reflection was recorded on a short time scale every 15 min (Figure 7a), showing that the relaxation occurs quite fast and immediately after workup of the sample. More precise data were obtained recording a full pattern with longer counting times of a sample containing the two phases with an average composition $Li_{0.65}Cr_4TiSe_8$ (Figure 7b,c). The first pattern was recorded immediately after intercalation and the second after 6 weeks storage time in an Ar glovebox. Obviously, the trigonal lattice parameters of the initial state are larger than in the relaxed state. The composition of the sample is not affected during relaxation. Rietveld refinement of the data shows that the unit cell volume of the trigonal phase shrinks by 2.4% during the 6 weeks relaxation, while the lattice parameters of the monoclinic phase seem not to be significantly affected (Table 2). But careful analysis of the atomic coordinates reveals some pronounced changes in the monoclinic phase. Immediately after the intercalation was stopped the M1−M3 bond as well as the M2−M2 distance are shorter than in the host material (Table 2). But after 6 weeks relaxation time the two separations M2−M2 and M2−M3 are longer than before, and also M1−M3 is expanded but without reaching the value in the monoclinic starting material. We note that the intralayer M2−M3 and M2−M2 separations of the relaxed monoclinic phase are near the M−M distance found for the relaxed trigonal phase (Table 2). It can be assumed that an electron transfer to M atoms of the monoclinic host is responsible for the alterations of interatomic M−M distances. Relaxation processes in the trigonal intercalated phase may be responsible for the observation that the lattice parameters slightly decrease at long intercalation, as seen in Figure 4, because intercalation and relaxation have opposed effects onto the lattice parameters.

A possible explanation for the relaxation processes is that different fractions of the starting material are intercalated to a different degree. Due to slow Li diffusion the surface regions of the host crystallites are assumed to exhibit a higher Li content than the inner domains. The relaxation is then a homogenization of the Li distribution in the grains. Some Li ions might also reside in tetrahedral sites in the freshly intercalated material which then move to more favorable octahedral sites during the relaxation process.

The relaxation process is governed by the Li diffusion from the Li-rich trigonal to the Li-poor monoclinic domains of the sample. According to the Rietveld data the trigonal fraction of the $Li_{0.65}Cr_4TiSe_8$ sample increases during the 6 week relaxation from 45.7 to 51.4%. This leads to a partial deintercalation of the trigonal domains on average. As a consequence the trigonal cell shrinks, which is evidenced by the smearing of the Bragg peaks to higher angles and results in very broad reflection profiles, as can be seen in Figure 7c. A fully equilibrated single-phase sample of the composition $Li_{0.75}Cr_4TiSe_8$ was obtained by the procedure described above, and the Rietveld data are also given in Table 2. It can be seen that despite the lower Li content the trigonal cell volume of the biphased sample after 6 weeks of relaxation is still larger than that of the equilibrated sample. It can be assumed that the full equilibration of the biphased samples is kinetically hampered at room temperature.

The remarkable elongation of the M−M distances in the monoclinic phase upon relaxation refers most probably to electronic effects that are due to the transfer of electrons that happens simultaneously with the homogenization of the Li distribution. Due to the fact that the lattice parameters do

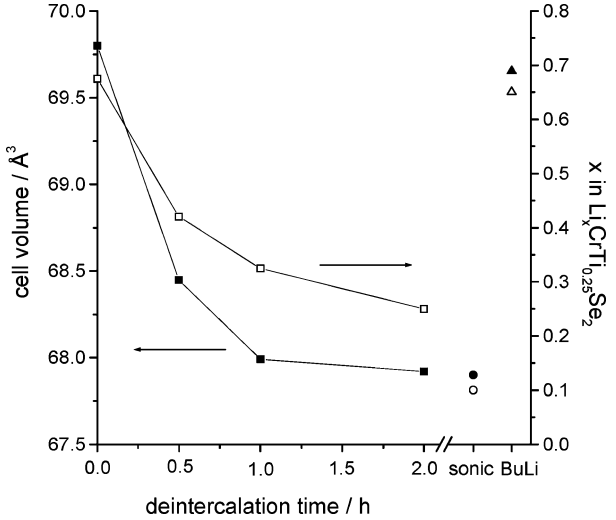

Figure 8. Time dependence of x' and the cell volume of $Li_{x'\approx0.75}CrTi_{0.25}Se_2$ during the deintercalation reaction in water. Cell volumes are results of Rietveld refinements (full symbols). The parameter x' was determined with AAS (open symbols). The sample marked "sonic" on the abscissa was exposed to ultrasonic after several days of deintercalation time (circles). A deintercalated sample was re-intercalated in BuLi, and the results are marked "BuLi" on the abscissa (triangles). The lines are guides for the eyes.

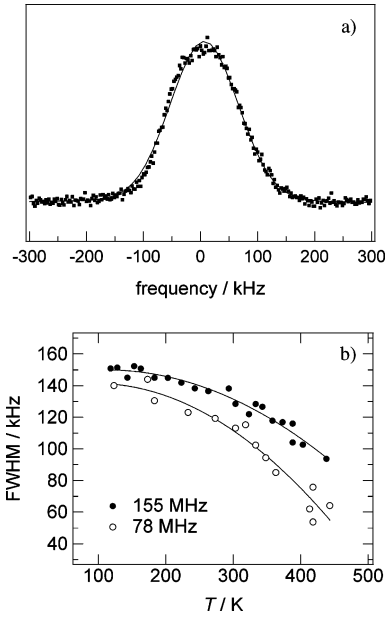

Figure 9. (a) ^{7}Li NMR spectrum of $Li_{2.8}Cr_4TiSe_8$ obtained from a static measurement at 293 K and a central frequency of 155 MHz. (b) Spectral width (full width at half-maximum, fwhm) vs temperature for central frequencies of 78 and 155 MHz.

not change significantly, steric effects of the Li^+ can be neglected.

Intercalation is a reversible process and deintercalation of $Li_{x'\approx0.75}CrTi_{0.25}Se_2$ was performed treating the intercalated phase with water. One important question was whether the symmetry changes back from trigonal to monoclinic when Li is removed from the intercalated phase. Whereas the AAS measurements showed that the Li content is drastically reduced after the treatment with water (Figure 8), the XRD measurements revealed that the symmetry is not switched back to monoclinic. The removal of Li from the trigonal $Li_{x'}CrTi_{0.25}Se_2$ phase introduces a structural contraction. The Rietveld refinements of the powder patterns of different samples after a water treatment for a certain time yield a decrease of the unit cell volume of 1.9 Å^3 which is almost 3% (Figure 8). Storing the intercalated material several weeks in water with intermittent ultrasonication led to an intercalated phase with composition $Li_{0.1}CrTi_{0.25}Se_2$. It can be assumed that the remaining small amount of Li is necessary to stabilize the trigonal symmetry and it is the lower compositional limit of the intercalated phase.

The re-intercalation of a deintercalated sample was performed at room temperature with BuLi in an Ar atmosphere. With increasing time the Li content is raised and the unit cell parameters are enlarged, demonstrating the reversibility of the intercalation reaction (compare Figure 8).

Finally we want to comment on the important question of whether the symmetry change is due to geometric effects or driven by electronic factors. The empty octahedral sites in Cr_4TiSe_8 are not too large for the Li^+ ions. Hence, intercalation of Li should have only a moderate geometrical influence on the crystal structure. On the other hand, during the intercalation process electrons are transferred from the guest to the host lattice. Such a change of electron density may be the reason for a structural change. An important experimental result is the fact, that Li cannot completely be removed from $Li_{0.75}CrTi_{0.25}Se_2$. The final composition after deintercalation was about $Li_{0.1}CrTi_{0.25}Se_2$ in all experiments, independent of the starting value of x. These experimental findings highly suggest that structural defects are not the main effect which might hinder the out-diffusion of Li during deintercalation. Hence, the most plausible explanation for the structural phase transition is the electron transfer to the host rather than the steric impact of the small Li^+ cations. On the other hand the electron transferred from Li to the host material is necessary to preserve the trigonal symmetry of $Li_xCrTi_{0.25}Se_2$ phases. It should be noted that compounds with the formal composition $M_{5+y}Se_8$ (M = Cr, Ti; $y \geq 0.1$) with a metal content higher than the 5/8 ratio for metal/selenium crystallize in the space group $P\bar{3}m1$ with axes very similar to those observed for $Li_{x'}CrTi_{0.25}Se_2$.[37]

NMR measurements were performed on ^{7}Li to elucidate the local structure around these probe nuclei. Static measurements were done at central frequencies of 78 and 155 MHz in the temperature range from 120 to 450 K. Figure 9a shows exemplarily the spectrum obtained at 155 MHz and 293 K. The spectrum reveals one broad peak without substructure which is Gaussian shaped and shows an overall width of 140 kHz (full width at half-maximum). Such a rather large width is typical of paramagnetic materials[38] and is due to the dipolar coupling of the nuclear spins of the Li ions with the electronic spins of the Cr ions. This is confirmed by the temperature and field dependence of this line width, which decreases continuously with increasing temperature and increases with increasing magnetic field (Figure 9b).

Further insight is obtained by ^{7}Li MAS NMR spectra which are shown in Figure 10 for temperatures of 310 and 360 K. They exhibit two subspectra which reveal the presence of two nonequivalent Li sites. The two peaks

(37) Lühmann, H. Diploma Thesis, University of Kiel, Germany, 2002.
(38) Grey, C. P.; Dupré, N. *Chem. Rev.* **2004**, *104*, 4493.

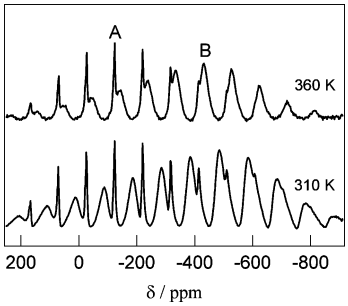

Figure 10. ^{7}Li MAS NMR spectra of $Li_{2.8}Cr_4TiSe_8$ at 310 and 360 K. Spectra were obtained at a ^{7}Li frequency of 155 MHz and a spinning rate of 15 kHz.

marked with "A" and "B" are the isotropic peaks. The first one has an isotropic chemical shift of −123 ppm, and the second one shifts with temperature from −430 ppm at 360 K to −487 ppm at 310 K. The large negative chemical shifts are caused by Fermi-contact interaction of the Li nuclei with the electron density of the unpaired Cr electrons. Strong dipole−dipole interactions between the nuclear spins of the Li ions and the electronic spins of the Cr ions lead to broad spinning sideband manifolds, which is consistent with the large width of the spectra obtained for the static measurements (Figure 9a). Comparison of the two subspectra reveals that the site marked with B shows much stronger coupling to the Cr ions, which becomes apparent in three different features: (i) the absolute value of the chemical shift is larger by a factor of about 4, (ii) its chemical shift exhibits a strong temperature dependence with larger absolute values at lower temperatures, and (iii) the central line and the spinning sidebands are much broader. Interestingly ^{7}Li MAS NMR measurements on a sample where part of the Cr ions are replaced by Ti, namely, $Li_{2.8}Cr_3Ti_2Se_8$,[39] show only the subspectrum A.

Acknowledgment. The financial support of this work from the state of Schleswig-Holstein, the Deutsche Forschungsgemeinschaft (DFG), and the Bundesministerium für Bildung und Forschung (BMBF) is gratefully acknowledged. We also thank Ron Siewertsen and Martin Wegner, who contributed to this work in their undergraduate studies project at the University of Kiel.

CM0518628

(39) Indris, S.; Wilkening, M.; Heitjans, P.; Wontcheu, J.; Behrens, M.; Bensch, W. To be published.